



Crystal structure of *Saccharomyces cerevisiae* cytoplasmic thioredoxin reductase Trr1 reveals the structural basis for species-specific recognition of thioredoxin

Zhenyi Zhang^{b,1}, Rui Bao^{b,1}, Yaru Zhang^b, Jiang Yu^a, Cong-Zhao Zhou^a, Yuxing Chen^{a,b,*}

^a Hefei National Laboratory for Physical Sciences at Microscale and School of Life Sciences, University of Science and Technology of China, Hefei, Anhui 230026, People's Republic of China

^b Protein Research Institute, Tongji University, Shanghai 200092, People's Republic of China

ARTICLE INFO

Article history:

Received 10 July 2008

Received in revised form 15 August 2008

Accepted 16 September 2008

Available online 1 October 2008

Keywords:

Thioredoxin

Thioredoxin reductase

Species-specific recognition

ABSTRACT

Thioredoxin reductase (TrxR) is a member of the pyridine nucleotide-disulfide oxidoreductase family of the flavoenzymes. It can use a dithiol-disulfide active-site to transfer reducing equivalents from NADPH to thioredoxin (Trx), via the cofactor FAD. In *Saccharomyces cerevisiae*, the cytoplasmic thioredoxin reductase Trr1 plays an important role in multiple cellular events under the control of transcription factor Yap1 and/or Rho5. Here we present the crystal structure of Trr1 at the resolution of 2.8 Å, the first fungal TrxR structure. Structural analysis shows it shares a very similar overall structure to *Escherichia coli* TrxR. However, fine comparisons indicate some distinct differences at the Trx recognition sites. These differences might be responsible to the species-specific recognition of Trx, which has been demonstrated by previous biochemical assays.

© 2008 Elsevier B.V. All rights reserved.

1. Introduction

Thioredoxin system, comprising thioredoxin (Trx), thioredoxin reductase (TrxR) and NADPH, is ubiquitously present in all organisms from prokaryotes to mammals [1,2]. In addition to its importance in oxidative stress defense, the thioredoxin system is also involved in regulating DNA synthesis, methionine biosynthesis, cell growth, gene transcription and apoptosis [3]. Reduced Trx functions as an electron donor for a wide range of proteins, including ribonucleotide reductase, protein methionine sulfoxide reductase and thioredoxin-dependent peroxidases et al. [4]. Oxidized Trx is in turn reactivated by TrxR, a member of the pyridine nucleotide-disulfide oxidoreductase family of the flavoenzymes [5,6]. This system uses a dithiol-disulfide active-site to transfer reducing equivalents from FAD (flavin adenine dinucleotide) to the downstream substrates [7].

Though the essential characteristics of Trx are conserved during evolution, two distinct types of TrxRs have evolved [8]. TrxRs from prokaryotes, yeast and plants have a subunit molecular weight (*Mr*) of 35 kDa, whereas those from *Plasmodium falciparum* and other higher eukaryotes have a subunit *Mr* of 50 kDa, due to addition of an extra domain at the C-terminus [9]. The two types of TrxR are distinctly different from both structural and functional points of view. The high *Mr* type TrxR is considered to be most likely evolved from glutathione reductase, which has three domains for one subunit, rather than TrxR of prokaryotes [10]. The active site is located at the NADPH binding domain in low *Mr* TrxRs, while at the FAD binding domain in high *Mr*

type. Furthermore, a large rotation of the NADPH binding domain in low *Mr* TrxRs is necessary for completion of the catalytic cycle [7], in contrast to a relatively rigid conformation of the high *Mr* TrxRs [8].

In *Saccharomyces cerevisiae*, an intact mitochondrial thioredoxin system (Trx3 and Trr2) is encoded in addition to its cytoplasmic counterpart (Trx1/Trx2 and Trr1) [11]. Trr1 and Trr2 share a sequence identity of 85% to each other, and both have the structural characteristics of TrxRs from lower organisms. Neither Trr1 nor Trr2 is essential for the viability of yeast, however, the *TRR1Δ* mutant shows extreme growth defects, very sensitive to H₂O₂ and high temperature, and methionine auxotrophic [12,13]. Trr1 plays an important role in multiple cellular events under the control of transcription factor Yap1 and/or Rho5 during oxidative stress [14,15].

In a frame to remodel the electron transfer route in thioredoxin systems at the atomic resolution, we have solved the structures of Trx1, Trx2 and Trx3 from *S. cerevisiae* [16–18]. Here we report the crystal structure of Trr1, representing the first fungal TrxR structure and another 3-D structure of low *Mr* TrxRs besides those from *Escherichia coli* [19], *Arabidopsis thaliana* [20], *Mycobacterium tuberculosis* [21] and *Helicobacter pylori* [10]. Comprehensive structural analysis indicates a couple of variations at the potential Trx binding sites compared to *E. coli* TrxR, which might contribute to species-specific recognition of Trx. Moreover, the structures of Trr1 and its substrates will provide us more insights into the inter-molecule electron transfer during oxidative stress.

2. Materials and methods

2.1. Protein expression and purification

The coding sequence of *TRR1/YDR353W* was amplified by PCR from the genomic DNA of *S. cerevisiae*. The PCR product was cloned into NotI

* Corresponding author. School of Life Sciences, University of Science and Technology of China, Hefei, Anhui 230026, People's Republic of China.

E-mail address: cyxing@ustc.edu.cn (Y. Chen).

¹ Both authors contributed equally to this work.

and NdeI restriction sites of the pET28b expression vector to add an N-terminal His-tag for affinity purification. The insert was verified by DNA sequencing. The resulting plasmid, was transformed to *E. coli* strain BL21 (DE3) (Novagen). Transformed cells were cultured at 37 °C in LB medium and incubated for 20 h at 18 °C with 0.2 mM IPTG on reaching OD₆₀₀=0.6. Cells were harvested by centrifugation, and resuspended in binding buffer (20 mM Tris-HCl, pH 7.5, 200 mM NaCl). After three cycles of freeze-thawing followed by sonication on ice, the lysate was clarified by centrifugation. The protein was purified using Ni-NTA affinity column (Qiagen) followed by size exclusion chromatography (Amersham Biosciences). The purity of protein was checked by SDS-PAGE. After exchanged into storage buffer (20 mM Tris-HCl, pH 7.5, 50 mM NaCl), protein was concentrated to 5 mg/mL using an Amicon Ultra 30 kDa cut-off concentrator (Millipore). The protein was then incubated with 0.5 mM NADPH and 0.1 mM FAD for half an hour and finally concentrated to 12 mg/mL, frozen in liquid nitrogen and stored at -80 °C until required.

2.2. Crystallization, X-ray data collection, structure determination and refinement

Prior to setting up crystallization experiments, Trr1 was incubated in freshly prepared 20 mM DTT. The initial crystallization conditions for Trr1 were obtained from the Crystal Screens I and II (Hampton Research Inc.), using the sitting-drop vapor-diffusion method. Each drop contained 1 μL reservoir solution and 1 μL protein sample. After optimization, yellow crystals at a maximal size of 300×50×10 μm³ were grown from drops comprising a mixture of equal volumes of protein (12 mg/mL) and reservoir solution containing 0.1 M MES buffer, pH 6.5, 10% PEG 20,000, using hanging-drop vapor-diffusion method after one week at 18 °C.

Trr1 crystal was flash frozen in mother liquor containing 18% (v/v) glycerol. Diffraction data were collected at 100 K on an in-house R-AXIS IV⁺⁺ image-plate detector using Cu Kα radiation (wavelength 1.5418 Å) generated with a Rigaku rotating-anode generator (operated at 50 kV and 100 mA) and focused with a confocal mirror. The data were indexed and integrated with MOSFLM and scaled using SCALA from CCP4 suit. The crystal belongs to the space group *P2*₁ with two molecules in an asymmetric unit. The 2.5 Å crystal structure of TrxR from *A. thaliana* (PDB code: 1vdc), which has 64% sequence identity to Trr1, was used as the initial search model. The molecular replacement was performed with Molrep of CCP4i. After refinement by Refmac, the model had an *R* factor of 22.6% and *R*_{free} of 23.4%. It contains all residues except for the first methionine in both subunits. PROCHECK finds 84.5% of the residues in the most favored regions and the rest in allowed regions. Data collection and refinement statistics are listed in Table 1. The final coordinates and structure factors have been deposited in protein data bank (<http://www.rcsb.org/pdb>) under the accession code of 3D8X.

2.3. Activity assay of *S. cerevisiae* Trr1 and Trr2 towards Trx3

The activity of *S. cerevisiae* Trr1 and Trr2 was determined by the DTNB assay, which was performed as described previously [22]. Briefly, the reaction mix contains 100 mM phosphate buffer, pH 7.0, 2 mM EDTA, 1 mM DTNB and 0.5 mM NADPH. The reaction containing 0.2–14 μM Trx3 were triggered by adding 10 nM Trr1 or Trr2. The absorbance at 412 nm was monitored for 10 min at 25 °C in a final volume of 200 μL (Beckman-Coulter DU800).

3. Results and discussion

3.1. Overall structure

The crystal structure of *S. cerevisiae* Trr1 was determined at the resolution of 2.8 Å using molecular replacement with the 2.5 Å crystal structure of *A. thaliana* TrxR (PDB code: 1vdc) as the search model. The final model contains 318 residues with two molecules in an asymmetric unit. One FAD molecule was incorporated in each subunit,

Table 1
Data collection and refinement statistics

Parameter	Values
<i>Diffraction data</i>	
Space group	<i>P2</i> ₁
Asymmetric unit	Dimer
Cell parameters <i>a</i> , <i>b</i> , <i>c</i> (Å), β (°)	54.23, 125.00, 60.97, 114.16
Resolution (Å) ^a	30–2.8 (2.91–2.8)
Total reflections	20,419
Unique reflections	19,676
<i>I</i> /σ	6.51 (1.60)
Completeness (%)	96.6 (95.3)
<i>R</i> _{sym} (%) ^b	15.3 (42.0)
<i>Refinement</i>	
Resolution	20–2.8 (2.87–2.8)
<i>R</i> _{cryst} (%) ^c	22.6 (31.2)
<i>R</i> _{free} (%) ^d	23.4 (34.3)
Protein atoms	4920
Solvent atoms	100
Average <i>B</i> (Å ²)	22.66
Rms deviation in	
Bonds (Å)	0.009
Angles (°)	1.223

^a The values in parentheses refer to the highest resolution shell of 2.91–2.8 Å.

^b $R_{sym} = \sum |I_i - \langle I \rangle| / \sum I_i$, where I_i is the intensity of a reflection, and $\langle I \rangle$ is the average intensity of that reflection.

^c $R_{cryst} = \sum ||F_{obs}| - |F_{calc}|| / \sum |F_{obs}|$.

^d 4.8% of the data was set aside for free *R*-factor calculation.

but the electron density of NADPH was not well defined. There was no continuous electron density for NADPH in subunit A, and very poor electron density in subunit B. Only the adeninyl ring and three phosphate groups of NADPH were finally incorporated in the final map of subunit A. The NADPH has been found to be disordered as in other pyridine nucleotide-disulfide oxidoreductase [23].

The yeast *S. cerevisiae* Trr1 forms a homodimer as other low *Mr* TrxRs. Sequence alignment shows that Trr1 shares a sequence identity of 50% and 64% with TrxRs of *E. coli* and *A. thaliana*, respectively (Fig. 1). The overall structure of yeast Trr1 resembles other known TrxR structures (Fig. 2). Superposition of the C_α atoms of Trr1 to *E. coli* TrxR and *A. thaliana* TrxR gives a root-mean-square deviation (RMSD) of 1.87 Å and 1.32 Å respectively. As with other low *Mr* TrxRs, each subunit of Trr1 has two similar Rossmann fold domains, the FAD binding domain (residues 2–123 and 251–319) and the NADPH binding domain (residues 127–250), separated by a large cleft. Each domain contains a central five-stranded parallel β-sheet with a three-stranded β-sheet on one side, and three α-helices on the other side. The two domains are connected by two stands, β7 and β16 (assigned to the FAD binding domain), and very few inter-domain contacts. The major interaction between the two domains is contributed by the isoalloxazine rings of FAD and the active cysteine residues in the NADPH binding domain. One hydrogen bond is formed between the amino hydrogen of Thr50 and the side chain of Gln136. The conserved Thr repeats region forms a hydrogen bond between the two domains in all TrxRs of known structure (Fig. 1).

In the dimer, the whole buried inter-subunit surface area is about 2214 Å² (Fig. 2). The majority of interface is contributed by the two FAD binding domains which cover an area of approximately 1565 Å². The NADPH binding domain of one subunit interacting with FAD binding domain of the other contributes to the rest of the interface. The dominant interactions are hydrophobic interactions, in addition to 23 hydrogen bonds formed by some polar residues.

The two active site residues Cys142 and Cys145 are located in the β8-α4 loop and helix α4 respectively (Fig. 2). The 2.03 Å distance between the two cysteine residues identifies that Trr1 is in oxidized form. The isoalloxazine ring of FAD packs against the disulfide bond at a distance of 3.15 Å. This conformation is referred to FO (flavin-

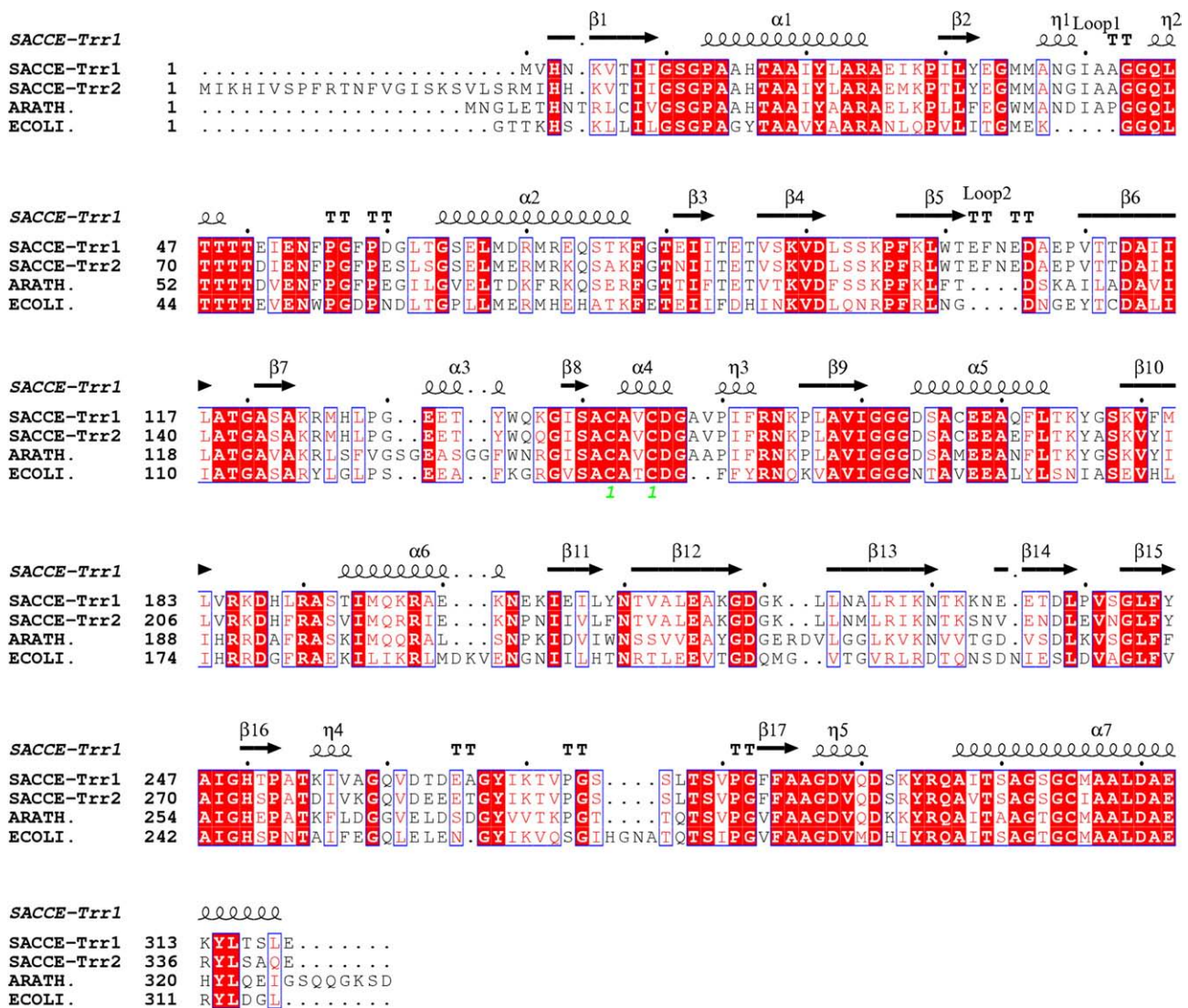


Fig. 1. Structure-based alignment of *S. cerevisiae* Trr1 and Trr2, and TrxRs from *A. thaliana* and *E. coli*. The sequence identities of Trr1 with the TrxRs of *A. thaliana* and *E. coli* are 50% and 63%, respectively. The secondary structure is for Trr1. The figure was produced with ESPript [30] based on an alignment by CLUSTAL X [31].

oxidizing) conformation, which allows the electrons transferred from FAD to disulfide. Just like the FO conformation in other TrxRs, S atom of Cys145 is close to the isalloxazine ring, while Cys142 is farther away. In this conformation, the active site is buried between the NADPH binding domain and the FAD binding domain, thus not accessible for Trx. A large rotation of NADPH binding domain is proposed to be necessary for exposing the active site, as found in *E. coli* TrxR [7].

3.2. Comparison with *E. coli* TrxR

The overall structure of Trr1 is similar to *E. coli* TrxR. When the FAD domains are superimposed, the NADPH domain of Trr1 is rotated by approximately 8° compared to the corresponding domain of the *E. coli* TrxR. However, this slight rotation is not enough for the active site of Trr1 to be exposed. This domain rotation was also found when comparing *A. thaliana* TrxR to *E. coli* TrxR, which has been proposed to be resulted from the dynamic behavior of low *Mr* type TrxR [20]. The RMSD of two corresponding domains between Trr1 and *E. coli* TrxR is 1.61 Å for FAD domain (183 C α atoms) and 1.86 Å for NADPH domain (121 C α atoms) respectively. The major differences of high RMSD occur in several loops, some of which are crucial for the Trx binding (for example, loop1 and loop2 showed in Fig. 1 and Fig. 4).

3.3. Thioredoxin binding site

The mechanism of the interaction between Trx and low *Mr* TrxR was speculated by many previous studies [24–27] and further confirmed by the crystal structure of *E. coli* Trx1–TrxR complex [7]. It has been proved that the NADPH domain of TrxR rotates a large angle for exposing the active site and a substantial surface, and makes itself interact with Trx. Comparison of *S. cerevisiae* Trr1 with *E. coli* TrxR shows very similar overall structure and the essential characteristics of the substrate Trxs are also conserved, but they still show species-specific recognition of Trx by TrxR. It has been demonstrated that *E. coli* TrxR can only reduce *E. coli* Trx1 and Trx2, and does not show any activity towards *S. cerevisiae* Trx3 [28]. In *S. cerevisiae*, although Trx2 only shares a 41% sequence identity with Trx3, they have very similar overall structure, especially at the region around the active site. Superposition of the structures of Trx2 [17] and Trx3 (manuscript in preparation) gives an RMSD is 1.23 Å between 102 C α atoms [17,18]. Activity assays indicated Trr1 can also reduce *S. cerevisiae* Trx3 at an efficiency similar to that of Trr2 (Fig. 3), although they are localized at different subcellular compartments. These results indicated that there is a very strong selectivity between the *E. coli* and yeast thioredoxin systems, whereas almost no selectivity between the two counterpart systems inside of the yeast.

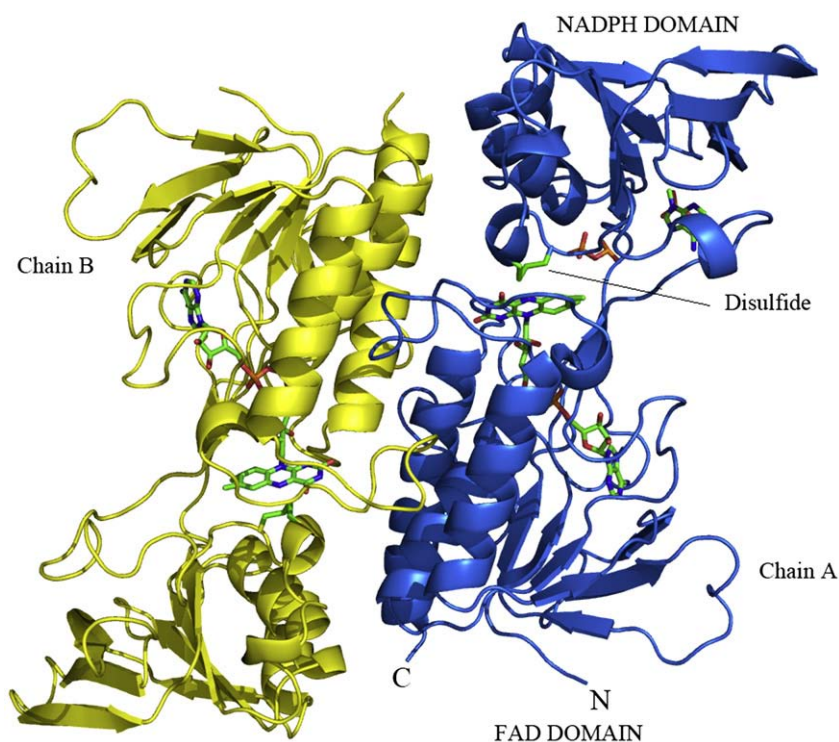


Fig. 2. Overall structure of Trr1 dimer. The FAD molecules, adenine ring and three phosphate groups of NADPH and the disulfides of active sites were drawn in stick model. This figure was produced by PyMOL [32].

To decipher the structural basis of this selectivity, we built a simulated model of Trr1–Trx2 complex based on the *E. coli* TrxR/Trx1 complex. Fine comparisons of the potential Trx binding regions of *S. cerevisiae* Trr1 with *E. coli* TrxR suggested some distinct differences at both FAD and NADPH binding domains. In the FAD binding domain, major differences were observed in two loops (loop1 and loop2) (Fig. 4). Loop1 of Trr1 is constituted of residues Glu33–Gly43 and loop2 comprises residues Thr101–Val110. Owing to insertion of residues (Gln–Gly–Ala–Ala for loop1, Glu–Phe–Gln–Glu for loop2) (Fig. 1), both loops are longer than those in *E. coli* TrxR. Residues of loop1 form two β -turns, which are conserved in lower eukaryotic TrxRs [20], while most prokaryotic proteins have a shorter loop. In the simulated complex model, loop1 of Trr1 was found to interact with the C-

terminal loop between $\beta 5$ and $\alpha 4$ of Trx2, mainly via hydrophobic interactions. Loop2 in fungal TrxRs is longer than that from other organisms, as shown in the sequence alignment of TrxRs (Fig. 1). Moreover, most insertion residues are negatively charged, and they give Trr1 a more negative potential surface around loop2 than *E. coli* TrxR. Two helices $\alpha 2$ and $\alpha 4$ of Trx2, opposite to loop2 of Trr1, possess positive charge owing to residues Lys43 and Lys97. These residues of complementary charge may be involved in protein–protein recognition between the two proteins. On the other hand, the C-terminal loop of *S. cerevisiae* Trx2 is shorter than that of *E. coli* Trx [7,17,29], which makes the C-terminal loop shift about 3.5 Å towards the core β sheet comparing to that of *E. coli* Trx1. The longer loops of Trr1 may be necessary to complement the shorter C-terminal loop of *S. cerevisiae* Trx. In addition, both loops have a higher B factors, indicating their flexibility.

In fact, the interactions between the NADPH binding domain and Trx1 are more important for recognition in the structure of *E. coli* TrxR–Trx1 complex [7]. A series of variations was also found in this domain. A loop of *E. coli* Trx1 (residues Tyr70 to Ile75) inserts into a complementary groove on the surface of TrxR NADPH binding domain, with side chain of Arg73 pointing to the bottom of the groove. But in *S. cerevisiae* Trx2, this Arg73 is substituted by Ser71 with a shorter side chain. On one side of the groove, two residues Phe141 and Phe142 of TrxR form a hydrophobic region fitting the hydrophobic pocket of *E. coli* Trx1. But in low *Mr* TrxRs, these two residues are replaced by four highly conserved residues Ala–Val–Pro–Ile which forms a short 3_{10} -helix after a truncated helix $\alpha 4$ in Trr1 (Fig. 4). On the other side of the groove, two residues Met215 and Arg130 of *E. coli* TrxR are substituted by Lys221 and Lys137 in Trr1. It makes Trr1 contains more positive charge at this side of the groove. And Lys 221 may interact with Glu69 of Trx2 (conserved in *S. cerevisiae* Trxs) through a salt bridge, which is not found in *E. coli* Trx1–TrxR complex [7].

In conclusion, the crystal structure of *S. cerevisiae* Trr1 which resembles the overall structures of *E. coli* TrxR, and other thioredoxin reductases of low *Mr*, provided us the structural basis that they could

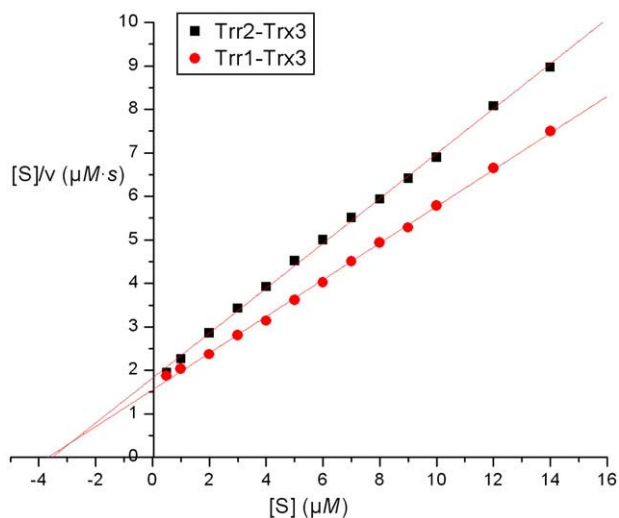


Fig. 3. Comparison of the activity of *S. cerevisiae* Trr1 and Trr2 towards Trx3, determined by DTNB assay [22]. The graph is drawn by Hanes–Woolf method, in which V_{max} is the reciprocal of the slope and the K_m is the negative X-axis intersect.

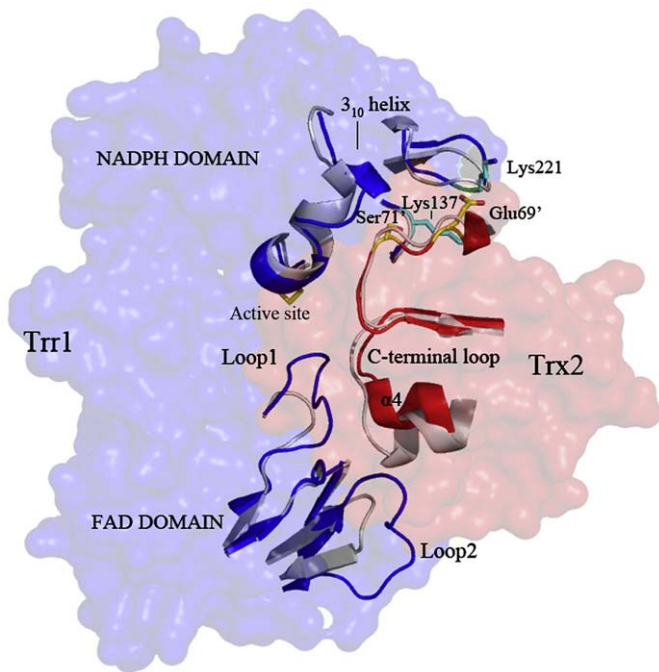


Fig. 4. The simulated model of yeast Trr1–Trx2 complex. Using the structure of *E. coli* TrxR–Trx1 complex (PDB code 1F6M) as a model, the NADPH binding domain (colored in blue) and FAD binding domain (colored in blue) of Trr1 are superimposed with the corresponding part of *E. coli* TrxR (colored in gray), respectively, and Trx2 (colored in red) is superimposed with *E. coli* Trx1 (colored in gray). The surface of the simulated Trr1–Trx2 complex model and the regions involved in recognition (as cartoon) are shown respectively. This figure was produced by PyMOL [32].

reduce the substrate thioredoxin by means of a similar mechanism. Comprehensive structural analysis and comparisons enable us find some variations at the potential Trx binding sites. The two loops of Trr1 at the Trx recognition interface are longer, and possess more residues of negative charge. The complementary shape and charge at the interface between yeast Trr1 and its natural substrate Trx1/Trx2 or paralog Trx3 could be determinants for their species-specificity. These findings are also in agreement with a series of combined biochemical activity assays performed in this study and the previous report [28].

Acknowledgements

This work was supported by the Ministry of Science and Technology of China (Projects 2006CB910202 and 2006CB806501), the Ministry of Education of China (Talents project of new century NCET-06-0374 and Program PRA B07-02 to YXC), and the National Natural Science Foundation of China (Programs 30670461 to YXC, 30470366 to CZZ).

References

- [1] E.S. Arner, A. Holmgren, Physiological functions of thioredoxin and thioredoxin reductase, *Eur. J. Biochem.* 267 (2000) 6102–6109.
- [2] A. Holmgren, Redox regulation by thioredoxin and thioredoxin reductase, *Biofactors* 11 (2000) 63–64.
- [3] T.A. Missall, J.K. Lodge, Thioredoxin reductase is essential for viability in the fungal pathogen *Cryptococcus neoformans*, *Eukaryot. Cell* 4 (2005) 487–489.
- [4] A. Holmgren, Thioredoxin, *Annu. Rev. Biochem.* 54 (1985) 237–271.
- [5] M. Luthman, A. Holmgren, Rat liver thioredoxin and thioredoxin reductase: purification and characterization, *Biochemistry* 21 (1982) 6628–6633.
- [6] C.H. Williams Jr., Thioredoxin–thioredoxin reductase—a system that has come of age, *Eur. J. Biochem.* 267 (2000) 6101.
- [7] B.W. Lennon, C.H. Williams Jr., M.L. Ludwig, Twists in catalysis: alternating conformations of *Escherichia coli* thioredoxin reductase, *Science* 289 (2000) 1190–1194.
- [8] L. Zhong, E.S. Arner, A. Holmgren, Structure and mechanism of mammalian thioredoxin reductase: the active site is a redox-active selenolthiol/selenenylsulfide formed from the conserved cysteine–selenocysteine sequence, *Proc. Natl. Acad. Sci. U. S. A.* 97 (2000) 5854–5859.
- [9] C.H. Williams, L.D. Arscott, S. Muller, B.W. Lennon, M.L. Ludwig, P.F. Wang, D.M. Veine, K. Becker, R.H. Schirmer, Thioredoxin reductase two modes of catalysis have evolved, *Eur. J. Biochem.* 267 (2000) 6110–6117.
- [10] T.N. Gustafsson, T. Sandalova, J. Lu, A. Holmgren, G. Schneider, High-resolution structures of oxidized and reduced thioredoxin reductase from *Helicobacter pylori*, *Acta Crystallogr. D Biol. Crystallogr.* 63 (2007) 833–843.
- [11] E.W. Trotter, C.M. Grant, Overlapping roles of the cytoplasmic and mitochondrial redox regulatory systems in the yeast *Saccharomyces cerevisiae*, *Eukaryot. Cell* 4 (2005) 392–400.
- [12] A.K. Machado, B.A. Morgan, G.F. Merrill, Thioredoxin reductase-dependent inhibition of MCB cell cycle box activity in *Saccharomyces cerevisiae*, *J. Biol. Chem.* 272 (1997) 17045–17054.
- [13] G.D. Pearson, G.F. Merrill, Deletion of the *Saccharomyces cerevisiae* TRR1 gene encoding thioredoxin reductase inhibits p53-dependent reporter gene expression, *J. Biol. Chem.* 273 (1998) 5431–5434.
- [14] O. Carmel-Harel, R. Stearman, A.P. Gasch, D. Botstein, P.O. Brown, G. Storz, Role of thioredoxin reductase in the Yap1p-dependent response to oxidative stress in *Saccharomyces cerevisiae*, *Mol. Microbiol.* 39 (2001) 595–605.
- [15] K. Singh, P.J. Kang, H.O. Park, The Rho5 GTPase is necessary for oxidant-induced cell death in budding yeast, *Proc. Natl. Acad. Sci. U. S. A.* 105 (2008) 1522–1527.
- [16] Y. Zhang, R. Bao, C.Z. Zhou, Y. Chen, Expression, purification, crystallization and preliminary X-ray diffraction analysis of thioredoxin Trx1 from *Saccharomyces cerevisiae*, *Acta Crystallogr. Sect. F Struct. Biol. Cryst. Commun.* 64 (2008) 323–325.
- [17] R. Bao, Y. Chen, Y.J. Tang, J. Janin, C.Z. Zhou, Crystal structure of the yeast cytoplasmic thioredoxin Trx2, *Proteins* 66 (2007) 246–249.
- [18] R. Bao, Y.X. Chen, Y. Zhang, C.Z. Zhou, Expression, purification, crystallization and preliminary X-ray diffraction analysis of mitochondrial thioredoxin Trx3 from *Saccharomyces cerevisiae*, *Acta Crystallogr. Sect. F Struct. Biol. Cryst. Commun.* 62 (2006) 1161–1163.
- [19] G. Waksman, T.S. Krishna, C.H. Williams Jr., J. Kuriyan, Crystal structure of *Escherichia coli* thioredoxin reductase refined at 2 Å resolution. Implications for a large conformational change during catalysis, *J. Mol. Biol.* 236 (1994) 800–816.
- [20] S. Dai, M. Saarinen, S. Ramaswamy, Y. Meyer, J.P. Jacquot, H. Eklund, Crystal structure of *Arabidopsis thaliana* NADPH dependent thioredoxin reductase at 2.5 Å resolution, *J. Mol. Biol.* 264 (1996) 1044–1057.
- [21] M. Akif, K. Suhre, C. Verma, S.C. Mande, Conformational flexibility of *Mycobacterium tuberculosis* thioredoxin reductase: crystal structure and normal-mode analysis, *Acta Crystallogr. D Biol. Crystallogr.* 61 (2005) 1603–1611.
- [22] A. Holmgren, M. Bjornstedt, Thioredoxin and thioredoxin reductase, *Methods Enzymol.* 252 (1995) 199–208.
- [23] P.A. Karplus, G.E. Schulz, Substrate binding and catalysis by glutathione reductase as derived from refined enzyme: substrate crystal structures at 2 Å resolution, *J. Mol. Biol.* 210 (1989) 163–180.
- [24] P.F. Wang, D.M. Veine, S.H. Ahn, C.H. Williams Jr., A stable mixed disulfide between thioredoxin reductase and its substrate, thioredoxin: preparation and characterization, *Biochemistry* 35 (1996) 4812–4819.
- [25] B.W. Lennon, C.H. Williams Jr., Reductive half-reaction of thioredoxin reductase from *Escherichia coli*, *Biochemistry* 36 (1997) 9464–9477.
- [26] S.B. Mulrooney, C.H. Williams Jr., Evidence for two conformational states of thioredoxin reductase from *Escherichia coli*: use of intrinsic and extrinsic quenchers of flavin fluorescence as probes to observe domain rotation, *Protein Sci.* 6 (1997) 2188–2195.
- [27] D.M. Veine, K. Ohnishi, C.H. Williams Jr., Thioredoxin reductase from *Escherichia coli*: evidence of restriction to a single conformation upon formation of a crosslink between engineered cysteines, *Protein Sci.* 7 (1998) 369–375.
- [28] J.R. Pedrajas, E. Kosmidou, A. Miranda-Vizuet, J.A. Gustafsson, A.P. Wright, G. Spyrou, Identification and functional characterization of a novel mitochondrial thioredoxin system in *Saccharomyces cerevisiae*, *J. Biol. Chem.* 274 (1999) 6366–6373.
- [29] M.F. Jeng, A.P. Campbell, T. Begley, A. Holmgren, D.A. Case, P.E. Wright, H.J. Dyson, High-resolution solution structures of oxidized and reduced *Escherichia coli* thioredoxin, *Structure* 2 (1994) 853–868.
- [30] P. Gouet, E. Courcelle, D.I. Stuart, F. Metz, ESPript: analysis of multiple sequence alignments in PostScript, *Bioinformatics* 15 (1999) 305–308.
- [31] J.D. Thompson, D.G. Higgins, T.J. Gibson, CLUSTAL W: improving the sensitivity of progressive multiple sequence alignment through sequence weighting, position-specific gap penalties and weight matrix choice, *Nucleic Acids Res.* 22 (1994) 4673–4680.
- [32] W.L. DeLano, The PyMOL Molecular Graphics System, DeLano Scientific, San Carlos, CA, USA, 2002.